In vitro digestion of emulsions: diffusion and particle size distribution using diffusing wave spectroscopy and diffusion using nuclear magnetic resonance

Maëla Choimet, Loïc Foucat, S. Marze

In Vitro Digestion of Emulsions: Diffusion and Particle Size Distribution using Diffusing Wave Spectroscopy and Diffusion using Nuclear Magnetic Resonance

Sébastien Marze, Maëla Choimet, Loïc Foucat

UR1268 Biopolymères Interactions Assemblages, INRA, F-44300 Nantes, France

ABSTRACT

Diffusing wave spectroscopy (DWS) is one of the few techniques enabling the investigation of structures and dynamics in turbid systems, that is in the multiple light scattering domain. This makes it an important technique to study colloidal dispersions such as foam, gel or emulsion. In this article, DWS in both back- and forward- multiple scattering was used to monitor the in vitro digestion of turbid undiluted emulsions. Eight formulations were tested using two triglycerides, two emulsifiers and two emulsifier concentrations.

The main goal of the study was to interpret the DWS data and compare the results to those from other techniques. We first extended the cumulants/moments fit method used for single scattering to obtain a particle size distribution (PSD) by DWS for multiple scattering. In the case of unimodal distributions, this compares well to PSD obtained from single scattering by dynamic light scattering (DLS). A second interpretation based on the multiple forward-scattering allowed the time-resolved diffusion coefficient to be measured. This was compared to diffusion monitored by nuclear magnetic resonance (NMR) of turbid undiluted emulsions. Both techniques report similar diffusion coefficients, although NMR measures a true molecular diffusion in different environments whereas DWS measures the diffusion of

supramolecular objects in the aqueous phase. These techniques are thus complementary, NMR resolving the kinetics of lipolysis, and DWS resolving the structural transitions, found to be first a droplet to vesicle one, then a vesicle to micelle one. In this study, the main formulation parameter influencing the digestion was found to be the type of triglyceride.

1. Introduction

The study of digestion, allowing foods to deliver nutrients and micronutrients, is a renewing field at the frontier of chemistry, physics and biology. From the chemistry point of view, it deals with multiple reactions, mostly enzymatic hydrolyses, but also redox and acid-base ones.[1] From the physics point of view, it deals with the digestive tract mechanics and the dynamics of multi-scale structures, usually in the colloidal form.[2] From the biology point of view, it describes the interactions with cells and with microbiota, mostly enterocyte absorption for cell transport.[3]

Combining all these sciences to study the interactions of the different processes in order to identify the controlling ones is challenging. It indeed requires multidisciplinary works and innovative experiments development allowing the nondestructive measurement of various properties.

In this context, we contribute by focusing on the combination of chemistry and physics of digestion. Our goal is to develop in vitro experiments giving insights on both aspects. In the past, digestion was indeed mostly studied as hydrolysis reactions (e.g. lipolysis). But there are now evidences that the multi-scales food structures influence digestion and bioavailability.[2,4,5]

A widely used model food system is emulsion, a liquid-liquid dispersion. It is minimally composed of lipid droplets dispersed in water and stabilized by an emulsifier at the oil/water interface (surfactant, protein, lipid…). But carbohydrates, dietary fibers and micronutrients (vitamins, minerals…) may be added to tend towards a real food.

Because of its dispersion nature, emulsion is turbid thus not easily characterized in a nondestructive manner. Most of the measurements are actually not made on the real emulsion, but on samples which need to be diluted or phase separated. This brings uncertainty concerning the preservation of the structures.

Nevertheless, some techniques are able to work directly on turbid systems. Many are based on multiple wave or particle scattering (light, sound, X-ray, neutron…) but only a few of them are available at the laboratory scale, like confocal microscopy and diffusing wave spectroscopy DWS (or its acoustic variant). Because it allows the study of structures in very turbid samples, DWS starts to spread for the characterization of food dispersions such as emulsion,[6] foam,[7] or gel [8]. A more developed laboratory technique based on atomic nucleus magnetism is nuclear magnetic resonance.[9] It classically resolves molecular characteristics but may also be used to study structures indirectly. Moreover, all those experiments are in principle able to resolve dynamics in dispersed systems.[10]

In this article, we report the exploration of DWS and NMR as nondestructive techniques to monitor the in vitro digestion of model emulsions. First we give some elements of the DWS theory and extend it to obtain a particle size distribution. Then we analyze the diffusion coefficients measured by DWS and NMR in order to interpret the digestion progress.

2. Materials and methods

2.a. Materials

Tricaprylin TC (T9126), triolein TO (T7140), sodium oleate NaO (O7501), decanal (W236209), sodium glycodeoxycholate NaGDC (G9910) and pancreatic lipase type II (L3126) were provided by Sigma-Aldrich France. β-lactoglobulin (βLG) was purified from whey protein isolate in our laboratory. In all preparations, Milli-Q water having an electrical resistivity of 18.2 $M\Omega.cm$ was used.

2.b. Emulsion preparation

Oil/water emulsions of dispersed oil volume fraction $\phi = 0.2$ were prepared the day of the in vitro digestion using a 7.5 $mg.mL^{-1}$ solution of either NaO or βLG (as emulsifier) in 10 *mM* NaH_2PO_4 buffer adjusted to pH 7.5 as the aqueous phase, and either tricaprylin or triolein (both containing 10 wt% decanal as a model micronutrient) as the oil phase. A total volume of 10 *mL* was placed in a 50 *mL* plastic vial, pre-emulsified for 2 *min* at 15000 *rpm* using a rotor-stator homogenizer (SilentCrusher M equipped with the 12F generator, from Heidolph Instruments, Germany). Immediately after, the pre-emulsion was sonicated using a Misonix Sonicator 4000 equipped with a microtip probe 419 (Qsonica, Connecticut, USA) for 2 *min*, alternating 15 *s* sonication and 15 *s* pause. A total of three cycles were performed with a 2 *min* pause between them to let the emulsion cool. The total energy brought to the emulsions was always about 1.8 *kJ*.

All solutions were made by magnetic stirring at ambient temperature for 30-60 *min* and adjusted to pH 7.5 the day of the in vitro digestion. Only the dissolution of NaO in water was stirred at 37±0.5 °C overnight and the high resulting pH brought back to 7.5 with addition of *μL* amounts of 1 *M* HCl (see [11]).

2.c. Emulsion digestion

The day of the in vitro digestion, an intestinal solution of 20 $mg.mL^{-1}$ NaGDC (bile salt) and 1 $mg.mL^{-1}$ pancreatic lipase was made in 130 *mM* NaH_2PO_4 buffer and adjusted to pH 7.5. The variants we called "+" for excess were obtained by adding 12 $mg.mL^{-1}$ of either NaO or βLG to this solution, corresponding to the NaO or βLG emulsion respectively. The role of these variants was to add excess emulsifier in the bulk, as the initial emulsions were formulated so that most emulsifier be adsorbed at the oil/water droplet interface.[12]

First 2 *mL* of emulsion was placed in a plastic vial and diluted in 130 *mM* NaH_2PO_4 buffer alone with a volume ratio 1:1 to mimic the gastric dilution, then in the intestinal solution with

a volume ratio 1:1 to start the digestion (the progressive increase of the emulsion ionic strength was designed to avoid flocculation during dilution[12]). The plastic vial was closed and placed in a Thermocenter oven (SalvisLab, Switzerland) at 37±0.5 °C on a magnetic stirrer Multipoint HP15 (Variomag, Germany) in the shake mode at 100 *rpm*. The final emulsions had a ionic strength of 100 *mM*, a pH of 7.5 and a dispersed volume fraction of 0.05 for a total volume of 8 *mL*. They contained 10 $mg.mL^{-1}$ NaGDC and 0.5 $mg.mL^{-1}$ pancreatic lipase and either 1.5 or 7.5 $mg.mL^{-1}$ emulsifier, in the normal or in the excess (+) case respectively.

2.d. Nuclear magnetic resonance

All measurements were done on ^{1}H protons using a Bruker Avance DRX 400 *MHz*. The probehead was a 5 *mm* Diff30L with a maximum gradient strength of 1200 $G.cm^{-1}$ in the z direction (Bruker BioSpin, France). A PFGSE (Pulsed Field Gradient Spin-Echo, see [9]) sequence was developed for diffusion measurement, using 16 gradient strengths ranged linearly from 15 to 300 $G.cm^{-1}$, a diffusion time of 5 *ms*, and a repetition time of 10 *s* for a total acquisition time of 40 *min*. Data treatment was done with the TopSpin software (v2.1).

All 150 μL samples were placed in a 5 *mm* NMR tube and maintained at 37±0.1 °C. Reference spectra were obtained to identify the peaks of the pure triglycerides and the intestinal solution diluted 2-fold in 100 *mM* NaH_2PO_4 buffer. The day of the in vitro digestion, a sample from the emulsion was diluted 4-fold in 130 *mM* NaH_2PO_4 buffer to measure a reference. Then, the in vitro digestion was initiated on another emulsion sample diluted as described in 2.c, and monitored in the NMR device by running diffusion measurements for about 24 hours, with a 20 *min* pause between acquisitions.

NMR measurements were performed on 2 independent digestions for TC-βLG, TC-NaO+ and TO-βLG+ and showed very good repeatability (see the results section). So, for the other emulsions, only one digestion was performed.

2.e. Laser diffraction

The surface-based particle size distribution (PSD) of the freshly made emulsions was measured by laser diffraction (LD) using a Mastersizer S equipped with a 2 *mW* He-Ne laser of λ = 633 *nm* and the 300RF lens (Malvern Instruments Ltd., Worcestershire, UK). The detection limits are 0.05 and 900 μm. The refractive index n_0 of the aqueous phase was 1.335 and those of TC and TO were 1.445 and 1.465 respectively. The absorption was set to 0.001. Emulsions were diluted with distilled water in the dispersion unit to reach an oil volume concentration near 0.01 % for the circulation in the measurement cell. To check the effect of the ionic strength, other samples were pre-diluted 4-fold in 130 *mM* NaH_2PO_4 buffer before the dilution in the dispersion unit. Only the βLG emulsions showed a small increase of the PSD.

2.f. Dynamic light scattering

Contrary to the static methods where intensities at all angles are analyzed in the statistical equilibrium, DLS is based on temporal resolution of intensity of a single angle (respectively large or small for back- or forward- scattering). A typical device involves a laser as source and a single mode optical fiber as collector. The treatment of the collected photons is performed by a photomultiplier tube which emits electrons corresponding to each individual photon input. The output is then interpreted by a digital correlator in terms of intensity pulses I at different time intervals τ ranging from several *ns* to *ks*, from which temporal correlations are calculated. That is why DLS is also called photon correlation spectroscopy (PCS). A classical calculation is the intensity autocorrelation:

$$\frac{\langle I(\tau)I(0)\rangle}{\langle I(0)\rangle^2} = 1 + \beta.g_2(\tau) \qquad (1)$$

where < > defines an ensemble average, $g_2(\tau)$ is the intensity autocorrelation function (IACF) and β is a coefficient, depending on the collection optics, determined by imposing $g_2(0) = 1$.

Back-scattering IACF was obtained at 37±0.5 °C using a Zetasizer Nano ZS (Malvern Instruments Ltd., Worcestershire, UK) equipped with a 4 *mW* He-Ne laser of λ = 633 *nm*. The exact angle θ between the laser beam and the detector (avalanche photodiode) is 173°. The laser power is automatically attenuated to collect an optimal scattered intensity. The measurement position was set to the maximum of 4.65 *mm*, that is 3.65 *mm* inside the sample as we used disposable 12 *mm* square polystyrene cuvettes with 1 *mm* thick walls (Brand, Wertheim, Germany). The optical properties were the same as previously for laser diffraction. A 30 *s* acquisition was generally enough to obtain a stable IACF.

30 μL of the final emulsion was diluted in 1.5 *mL* of 100 *mM* NaH_2PO_4 buffer, of which 1 *mL* was placed in a capillary cell (DTS1060) at 37±0.5 °C so that the digestion directly occurred in the measurement cell. The IACF was recorded automatically every 2 *min* to continuously monitor the effect of digestion.

For the initial emulsions, the volume-based PSD obtained using the Zetasizer Nano ZS and the surface-based PSD obtained using the Mastersizer S were found to be the closer representations, and are thus used in this article.

The PSD of the intestinal solution with or without the emulsifier excess was also measured by DLS as 100 μL diluted in 1 *mL* of 100 *mM* NaH_2PO_4 buffer.

2.g. Diffusing wave spectroscopy

To obtain IACF in undiluted samples, we used a homemade DWS equipment. The measurement principle and components are essentially the same as those of DLS. However, because there is multiple scattering, light leaves the sample in every directions, so the power of the laser has to be much higher than for DLS in order to collect enough light in a particular direction. We thus use a 100 *mW* DPSS laser of λ = 532 *nm* (LRS-0532-PFM-00100-03, Laserglow Technologies, Canada). In order to resolve short time intervals, we based our setup on the cross-correlation of the signals of two independent photomultiplier tubes, obtained by

splitting the beam collected by a single collimated optical fiber aligned at λ = 532 *nm* (CFS18-532-FC, Thorlabs, France). The photomultiplier tubes (Hamamatsu HC120-08), the beam splitter, the electronic correlator (Flex02-01D) and the analysis software were supplied by Correlator.com (Bridgewater, NJ, USA). Both back- and forward- scattering geometries can be set by changing the position of the collimated optical fiber.

3 *mL* of digesting emulsion was taken each hour from the plastic vial in the oven and transferred in a closed disposable 12 *mm* square polystyrene cuvette. This was set for measurements on a hotplate at 37±1 °C with no stirring (IKAMAG RT5power, IKA, Germany). Depending on the geometry and the sample turbidity, the acquisition time lied between 30 *s* and 10 *min* in order to obtain a good IACF. Both back- and forward- scattering geometries were used. After both measurements, the 3 *mL* sample was put back in the plastic vial in the oven.

At least 2, usually 3 independent emulsions, digestions and associated measurements were done on different days in order to check the overall repeatability of the study. The results are presented as averages and standard deviations, except if stated otherwise.

3. Light scattering theory

In this section, we review the interpretation of the IACF to obtain the PSD for single scattering,[13] then extend it to multiple scattering.

3.a. PSD for single light scattering

For single scattering by monodisperse diffusing particles with no absorption, the theoretical expression for the IACF is:

$$g_2(\tau) = \exp(-2\tau / \tau_0) \qquad (2)$$

where τ_0 is the characteristic decay time, given by $\tau_0 = 1/(q^2 D)$, D being the diffusion coefficient and $q = \frac{4\pi . n_0}{\lambda}\sin(\theta/2)$ the wave vector, with n_0 the refractive index of the dispersion medium. In the polydisperse case, it is a sum of exponentials such that:

$$\sqrt{g_2(\tau)} = \int_0^\infty C(\mathrm{T}).\exp(-\tau/\mathrm{T})\mathrm{dT} \tag{3}$$

Note that $\sqrt{g_2(\tau)}$ represents the electric field autocorrelation function $g_1(\tau)$. The recovery of the distribution C(T) is known as a mathematical ill-posed problem. It nevertheless can be solved using approximation methods with fitted parameters (cumulants, inverse Laplace transform, least-squares…), among which the cumulants fit is the most used:

$$\sqrt{g_2(\tau)} = \exp\left(-\tau/\mathrm{T}_m + \frac{1}{2!}\kappa_2.\tau^2 - \frac{1}{3!}\kappa_3.\tau^3 + \ldots\right) \tag{4}$$

$$g_2(\tau) = \exp\left(-2\tau/\mathrm{T}_m + \frac{2}{2!}\kappa_2.\tau^2 - \frac{2}{3!}\kappa_3.\tau^3 + \ldots\right) \tag{5}$$

where T_m is the mean decay time and κ the cumulants of the distribution. Usually, the third order is not used so there are only two fitting parameters.

Alternatively, using the relation between the cumulant-generating and the moment-generating functions $\exp\left(\sum_{n=1}^{\infty}\frac{\kappa_n.\tau^n}{n!}\right) = 1 + \sum_{n=1}^{\infty}\frac{\mu_n.\tau^n}{n!}$ to introduce the moments μ of the distribution gives:[14]

$$\sqrt{g_2(\tau)} = \exp\left(-(\tau/\mathrm{T}_m)\right)\left(1 + 0.5\mu_2.\tau^2\right) \tag{6}$$

$$g_2(\tau) = \exp\left(-2(\tau/\mathrm{T}_m)\right)\left(1 + 0.5\mu_2.\tau^2\right)^2 \tag{7}$$

the latter being more robust than (5) upon fitting at large τ. A polydispersity index Pi is defined as $Pi = \mu_2.\mathrm{T}_m^2$.

All fittings can be performed directly on size rather than time by substituting τ by d using $D = 1/(q^2 \tau)$ and the Stokes-Einstein (SE) relation $d = \frac{k_B.T_K}{3\pi\eta D}$, where k_B is the Boltzmann constant, T_K the temperature in Kelvin, and η the viscosity of the dispersion medium.

From the two parameters of the fitting of (5) or (7), a PSD can be obtained. For example, the form of a lognormal one is:

$$PSD = \frac{\exp\left(-0.5\left(\frac{\ln d - \ln d_m}{\ln(1+Pi)}\right)^2\right)}{\ln(1+Pi)\sqrt{2\pi}} \tag{8}$$

3.b. Diffusing wave spectroscopy theory

The theoretical background of DWS was published in 1990 by Pine et al..[15] The fundamental equation for diffusion of total light path length s is similar to that of single light scattering:

$$\sqrt{g_2(\tau)} = \int_0^\infty C(s)\exp\left(-2(\tau/\tau_1)(s/l^*)\right)ds \tag{9}$$

where $\tau_1 = 1/(k^2 D)$, with the wave number $k = 2\pi.n_0/\lambda$.

For diffusive motion of non-absorbing, non-interacting ($\phi < 0.1$) and monodisperse spheres, the IACF is widely described by a simplified form in back-scattering:

$$g_2(\tau) = \exp\left(-2\gamma\left(6\tau/\tau_1\right)^{0.5}\right) \tag{10}$$

with $\gamma = \frac{\langle z_0 \rangle}{l^*} + \frac{2}{3}$, where 2/3 is an empirical fitting parameter, l^* is the transport mean free path and $\langle z_0 \rangle$ is the averaged penetration depth into the sample, usually taken to be constant and close to l^* (between $2l^*/3$ and $4l^*/3$).

For diffusive motion of non-absorbing, non-interacting ($\phi < 0.1$) and monodisperse spheres, a simplified form of the IACF in forward-scattering (or transmission) is:

$$g_2(\tau) = \exp\left(-2\left(L/l^*\right)^2\left(\tau/\tau_1\right)\right) \tag{11}$$

with only one fitting parameter because L is the sample thickness (10 *mm* for our cuvette) and l^* can be known by an independent measurement or by the Mie theory.[16] Experimentally, l^* is deduced from samples of known mean diameter from (11) and from the measured transmitted intensity using the relation:

$$\frac{I}{I_0} = \frac{5l^*}{3L + 4l^*} \tag{12}$$

Using Mie theory, $l^* = \frac{(k.d)^4 k^2}{\pi\rho}\left(\int_0^{2k.d} F(x)S(x)\, x^3\, dx\right)^{-1}$, where $x = q.d$, $F(x)$ and $S(x)$ are the form and the structure factors and ρ is the number density of particles. This can be calculated as $l^* = 1/\left(\rho\sigma\langle 1-\cos\theta\rangle\right)$, where σ is the scattering cross-section.

Once all parameters are known in equation (10) or (11), the mean particle size is deduced from SE (using the water viscosity at the experimental temperature) with a correction on the measured diffusion coefficient to evaluate the value at zero volume fraction, found by Batchelor[17] to be $D_{meas} / D = (1 - 1.83\phi)$.

3.c. PSD for multiple light scattering

In this section, we extend the statistical analysis of the cumulants and moments to DWS.

In forward-scattering, we notice that (11) can be deduced from (2) by substituting τ by $\left(L / l^*\right)^2 \tau$. The same is done in (7) to give:

$$g_2(\tau) = \exp\left(-2\left(L / l^*\right)^2 (\tau / \tau_1)\right)\left(1 + 0.5\left(L / l^*\right)^4 \mu_2.\tau^2\right)^2 \tag{13}$$

with a polydispersity index Pi defined as $Pi = \mu_2.\tau_1^2$.

In back-scattering, the same principle is used with (10) and (2) by substituting τ by $\left(\gamma^2 6\tau\right)^{0.5}$ and τ_0 by $\sqrt{\tau_1}$. In (7), this results in:

$$g_2(\tau) = \exp\left(-2\gamma(6\tau / \tau_1)^{0.5}\right)\left(1 + 3\gamma^2 \mu_2.\tau\right)^2 \tag{14}$$

with a polydispersity index Pi defined as $Pi = \mu_2 . \tau_1$.

4. Results

4.a. Interpretation of the IACF

Figure 1 shows typical IACFs obtained by DWS during a digestion in both forward- and back- scattering. Those present two plateaus normalized to 0 and 1, the latter being well-resolved down to about 10^{-7} *s*. Below, after-pulsing generates an upward deviation which was not taken into account for the normalization. The IACF orders as a function of the digestion time, more clearly for forward- than for back- scattering. The IACF on the left always corresponds to the beginning of the digestion, and was thus used as reference. From the initial mean droplet diameter, as measured by LD (see section 4.f. for the values), we deduced the initial l^* or γ using (11) or (10) for forward- or back- scattering respectively.

For forward-scattering, we used (12) and the measured transmitted intensity to deduce l^* for the next measurements. Each l^* was first used to estimate the dispersed volume fraction ϕ considering an inverse proportionality between these quantities using the Mie theory. This is acceptable because this theory also predicts that l^* only slightly depends on the droplet diameter in the range explored in our experiments.[16] The estimated volume fraction was then used to apply the Batchelor correction to the diffusion coefficient. Finally, l^* and the corrected diffusion coefficient were used in (11) to deduce the size from the IACF.

The same procedure was applied to the back-scattering IACF except there is no intensity relation to deduce the next γ from the reference γ. To do so, we used (10) to find γ from a TO-βLG emulsion of known mean droplet diameter at 100 *mM* ionic strength for different dispersed volume fractions. As shown in figure 2, we found that γ is proportional to ϕ, so we used this relation to deduce γ from ϕ as measured by forward-scattering. This means that the interpretation of the back-scattering measurements is only possible if corresponding forward-

scattering measurements are performed to access ϕ (or any other technique accessing the dispersed volume fraction).

4.b. PSD for multiple light scattering

The procedure above was applied except we used (14) or (13) instead of (10) or (11) to fit the DWS back- or forward- scattering IACF respectively. Instead of one, the fittings provided two parameters, the mean droplet diameter and the second moment.

We first check the validity of this approach by applying it at 20 °C to monodisperse polystyrene particles dispersions of $\phi = 0.018$ and $d = 500$ *nm* (ref 95585, Fluka) and of $\phi = 0.032$ (diluted to $\phi = 0.016$) and $d = 200$ *nm* (ref 95581, Fluka). From DLS, we found a volume-based mean diameter of 525 and 202 *nm* respectively. We used these values in (14) or (13) to extract γ and μ_2 or l^* and μ_2 from DWS measurements. Figure 3 shows a comparison of the PSD obtained by DLS or using (8) for DWS. The agreement is very good, meaning the polydispersity values are similar. The extracted l^* for the 500 and 200 *nm* dispersions were respectively found to be of 155 and 160 μm, close to the theoretical Mie values of 130 and 135 μm calculated using phpMie (http://zakharov.zzl.org/lstar.php). The extracted γ were respectively found to be of 2.7 and 2.5 (± 0.05), a bit higher than previously reported.[16] The relation to the dispersed volume fraction was tested using the 200 *nm* dispersion, found to be sub-linear (power-law of figure 2), also found in other data.[18-19]

The procedure was applied to the digested emulsions. Figure 4 shows an example for the comparison of the lognormal PSD calculated using (8) with the DWS parameters, and the volume-based PSD from the DLS measurements. The results are in fairly good agreement with the limitation that back-scattering tends to overestimate the polydispersity whereas forward-scattering tends to underestimate it. Back-scattering is also more sensitive than forward-scattering to small sizes that develop during digestion. This is a known result in the Mie theory framework.[16] The reference γ value (at $\phi = 0.05$) in this example is 1.45. It is a bit

high compared to the values in figure 2 in 100 *mM* NaH_2PO_4 buffer alone. This is because there is a higher dispersion of the reference γ in digestion conditions. Nevertheless, the average reference γ is 1.25 ± 0.2, independently of the type of emulsion. This lies within the linear curve in figure 2. The l^* values will be given in the discussion section.

4.c. Diffusion from the forward-scattering DWS

Another way to interpret the IACF once the parameters are known is to plot the time-resolved diffusion coefficient. In the DWS theory framework, this is only valid in the forward-scattering case.[16] The diffusion coefficients are analytically calculated from the experimental IACF values for each time interval using (11) with $\tau_1 = 1/(k^2 D)$. Figure 1 shows the result of this calculation for the forward-scattering IACFs down to the time interval from which these start to exceed unity. Note that two values stand out in these curves: the maximum at short time-scales and the plateau value at intermediate time-scales.

4.d. Spectrum and diffusion from NMR

An example of some NMR spectra during digestion is shown in figures 5-6. Each peak was assigned to specific protons on the lipid molecules using letters, as shown in figure 5. The peaks were not shifted during emulsion digestion, because each initial triglyceride and its digestion products share most of their chemical groups. Nevertheless, some minor peaks tended to merge with the major ones, which resulted in less resolved spectra, but still in agreement with each pure triglyceride main peaks. Throughout the digestion, we thus measured the diffusion for the well defined peaks E, G and J. Those corresponds to the terminal CH_3 (J) and some CH_2 in the alkyl chains (G and E). Diffusion coefficients were determined for these 3 main lipid peaks, and an average was calculated. The diffusion coefficient of water was also determined.

We intended to study the decanal as a model micronutrient because its peak at 9.7 *ppm* was isolated and far enough from the water peak, but it revealed too small for a diffusion analysis.

We can only notice that it always decreases during digestion, which can mean that its diffusion coefficient increases as digestion progresses, or that decanal reacts during digestion. Some other minor peaks appeared during digestion, like the one around 3.7 *ppm*, which is specific of diglyceride and monoglyceride.

The initial water diffusion coefficient in the emulsions was found to depend only on the presence or absence of excess emulsifier, of $(2.54\pm0.02).10^{-9}$ $m^2.s^{-1}$ or $(2.67\pm0.03).10^{-9}$ $m^2.s^{-1}$ respectively. It was found to decrease as digestion progresses, the variation depending only on the triglyceride, of about 5% for TC and about 10% for TO.

4.e. Diffusion using DWS and NMR

NMR measurements reveal diffusion at the molecular scale. Such a small length-scale is reachable only at short time-scales using DWS. We thus report the maximum diffusion coefficient measured by DWS and compare it to the NMR lipid one. Those are shown in figures 7-8. Globally the ranges are similar, but DWS values display much higher deviations than the NMR ones. This high deviation is due to fluctuations at short time-scales but the average values within these fluctuations are actually close for the repetition of independent digestions (at least 2). As the digestion progresses, the techniques diverge, what we will interpret in the discussion section.

4.f. Monitoring of droplet size by DLS

Figure 9 shows the DLS volume-based mean droplet diameter versus the digestion time. LD surface-based values for the initial emulsions are included for comparison. Given the deviations, the freshly made emulsions have a similar mean droplet diameter except TC-NaO(+) for which it is significantly smaller. Also, DLS and LD values are in agreement, although the average values are overestimated by DLS for the TO emulsions (see figure 9 legend). Comparing the size evolution, the significant effects are those of the triglyceride and of the emulsifier type but no effect is seen with an excess of emulsifier. After 6-7 hours of

digestion, the emulsions reach a similar diameter only depending on the triglyceride, of 40 ± 2 *nm* for TC and 54 ± 4 *nm* for TO, corresponding to the lowest size population of the PSD (see figure 4).

These values should be compared to the mean diameters measured in the intestinal solution with or without the emulsifier excess. Those are 1.9 ± 0.8 *nm* in the intestinal solution alone, 2.5 ± 0.8 *nm* in the presence of excess βLG and 5 ± 0.5 *nm* in the presence of excess NaO. These are typical values for simple and mixed micelles.[20-21] The higher values at the end of the digestion mean either the droplets digestion is incomplete, or other objects than micelles formed, such as vesicles.[21-22]

5. Discussion

5.a. PSD for multiple light scattering

Equations (14) and (13) we derived to deduce PSD from the DWS back- or forward-scattering IACF respectively are especially efficient for the monodisperse polystyrene dispersions. For an unimodal distribution of a polydisperse emulsion (figure 4), they are still acceptable. When a bimodal distribution exists (figure 4, 5h), they are very limited, only reflecting one population (forward DWS) or an average of two populations (back DWS). A CONTIN procedure might be more suitable in this case.[23] Forward-scattering is also more convenient than back-scattering, as the intensity equation (12) to deduce l^* is more robust than a calibration curve based only on the dispersed volume fraction to deduce γ. Pine et al.[15] showed that γ depends on light polarization, scattering anisotropy, particle size and volume fraction, and reported γ between 1.5-3. However, $\frac{\langle z_0 \rangle}{l^*}$ values as low as 0.2 (see [18]) or as high as 4.6 (see [24]) were also measured. γ values of 0.1 or below were even found in strongly interacting systems depending on light polarization, colloidal state and volume fraction.[19] We

confirmed the volume fraction effect and also showed that γ depends on the type of dispersion (monodisperse polystyrene vs. polydisperse emulsion). Thus, to reach a fully quantitative back-scattering method, this parameter has to be investigated in detail for different dispersions.

5.b. Diffusion coefficients

The diffusion coefficient of figure 1 decreases as a function of the time interval. This is a typical result when obstacles induce an anomalous diffusion.[25] This is equivalent to the mean square displacement vs. time displaying a sub-linear log-log slope, found for many dispersions,[26] meaning the longer the time period, the more probable some particles collide thus slow each others. In our case of polydisperse emulsions, we also suspect that the different characteristic sizes appear in this time-resolved diffusion coefficient curve, down to the molecular scale.[16]

First we interpret the plateau value at intermediate time-scales. The diffusion coefficient is read and the corresponding diameter is calculated using SE. The diameters are in good agreement with those from the fitting of (11), meaning that the object corresponding to this plateau is the droplet.

Then we interpret the diffusion coefficients plotted in figures 7-8. To do so, we make different hypotheses about their possible origins. Each hypothesis is tested by calculating the corresponding diffusion coefficient using SE. Such a comparison is needed because there are only a few articles in the literature concerning the NMR measurement of diffusion in evolving emulsion,[27-28] and only two related to digestion.[29-30]

For the NMR measurements, the beginning of the digestion likely corresponds to the self-diffusion of a single triglyceride in a triglyceride environment TG/TG (TC and TO are practically insoluble in water). This was calculated using the viscosity at 37 °C for TC (12.8 *mPa.s*, see [31]) and TO (39.9 *mPa.s*, see [32]) and estimating the molecular diameter for a sphere

geometry using[33] $d = \left(\frac{6.M}{\pi.\rho_m.N_A} \right)^{1/3}$, where M and ρ_m are the molecular mass and density of the molecule and N_A is the Avogadro constant. The density at 37 °C of TC and TO are 0.938 $g.cm^{-3}$ (see [31]) and 0.899 $g.cm^{-3}$ (see [32]) respectively.

There are more possibilities for the long term digestion. Micelles are known to form,[34] so it could correspond to the self-diffusion of a single fatty acid in a fatty acid FA/FA (simple micelles) or in a fatty acid+bile salt (mixed micelles) environment (neglecting monoglyceride). It could also be the diffusion of a single FA in an aqueous environment FA/W (especially for TC). Diffusion coefficients were calculated as above using the viscosity at 37 °C for caprylic acid CA (4 *mPa.s*, see [35]) and oleic acid OA (17.7 *mPa.s*, see [36]) and the density at 37 °C for CA (0.897 $g.cm^{-3}$, see [35]) and OA (0.883 $g.cm^{-3}$, see [36]). We did not correct the value of the aqueous phase viscosity as a function of digestion time but it is possible using the water diffusion coefficient.

We report these calculated diffusion coefficients in figure 7. There is a very good agreement of the TG/TG hypothesis with the NMR diffusion coefficients in TO emulsions before the digestion, and an overestimation in TC emulsions. During the digestion, the diffusion of FA/W results in much too high diffusion coefficients. The FA/FA hypothesis is always in very good agreement with the NMR data. The mixed micelles hypothesis would probably result in similar estimations using a microviscosity (local viscosity in confined systems) instead of a bulk viscosity. Indeed, the microviscosity in micelles is typically reported between 4 and 20 *mPa.s* at 37 °C, depending on the chain lengths and mixture. [22,37-38] Fukuda et al.[22] also found that the microviscosities in OA micelles or vesicles are close. However, microviscosities for our exact systems were not reported, so the exact type of structure that forms can not be assessed from these diffusion coefficients. An intermediate hypothesis for which TG and FA coexist results in estimations lying between TG/TG and FA/FA. The

intermediate NMR data points thus likely represent a state where mostly lipolysis by lipase took place.

For DWS, although the initial diffusion coefficient is usually close to the one measured by NMR, it is unlikely to represent the TG/TG diffusion. DWS is indeed sensible to supramolecular objects dispersed in a continuous phase. So hypotheses should be made for the diffusion of droplets, vesicles or micelles in an aqueous environment. Using the mixed micelles diameters measured by DLS, we obtain diffusion coefficients that are in good agreement with the DWS ones for the long term digestion (M/W). Using the end plateau values measured by DLS (figure 9), we obtain diffusion coefficients that are in good agreement with the DWS ones at 1 hour of digestion (V/W). The DWS data points from this time to the end could thus represent a transition from vesicles (V/W) to mixed micelles (M/W). We confirmed this intermediate vesicular state in transmission electron microscopy and neutron scattering preliminary studies we are currently pushing further. In the literature, transitions were only reported for mixtures of phospholipids and bile salts so far.[39-40] The possibility of forming vesicles with various fatty acids is known without[41] or with[21] bile salts. However, this was never shown neither dynamically nor in emulsions.

Our results show that forward-scattering DWS can indeed be used to probe different characteristic sizes simultaneously. In the context of digestion of emulsions, the interpretation of the diffusion coefficients allows the monitoring of the evolution from an emulsified droplet system to a micellar system, through a vesicular one. In contrast, NMR probes the molecular mobility in different environments.

5.c. Digestion kinetics

We now analyze the role of the emulsion formulation on the evolution of the measured quantities during digestion. In addition to the parameters already shown, the forward-scattering DWS experiment provides l^*, from which the dispersed volume fraction is

deduced. These quantities are plotted in figure 10. We see that l^* may be close to L for some TC emulsions. In this case the multiple scattering hypothesis is no longer valid so the single scattering formalism should be used. Nevertheless, when l^* equals L, the timescales in (2) and (11) are simply related by the factor $4\sin^2(\theta/2)$. Because we work at small θ, the use of (2) results in droplet diameter or diffusion coefficient at least 2 orders of magnitude respectively below or above the ones found using (11). Such values strongly disagree with DLS or NMR ones, so a single scattering hypothesis is actually worst than a multiple scattering one.

The evolutions in figure 10 confirm that the TC emulsions are digested faster than the TO emulsions as already seen in figure 9. Given the deviations, the effect of the emulsifier type is not clear, depending on the overall formulation. The excess of emulsifier shows no effect, whatever the measurement is. Complementary experiments were performed to check those results and clarify the role of the emulsifier.[42] There are indeed contradictory results in the literature for whey protein isolate WPI (similar to βLG) and Tween (similar to NaO). Two articles report a minor effect on the digestion kinetics,[43-44] whereas others report a faster digestion with WPI compared to Tween[45] or with βLG compared to 2-monopalmitin.[46]

6. Conclusion

The interpretation of the DWS data allowed the PSD of undiluted emulsions to be obtained in both back- and forward- multiple scattering. This compared well with the PSD of diluted emulsions (single scattering) for unimodal distributions. In the contrary, for the long term digestion, the agreement was only partial, as bimodal distributions were usually seen by DLS. In this case, the cumulants/moments fit method developed here was not adapted, and a CONTIN procedure might give better results.

NMR diffusion measurements allowed the molecular evolutions to be followed, thus essentially the events related to lipolysis and the phase transfer. In complement, the time-

resolved diffusion coefficient derived from the forward-scattering DWS data allowed the simultaneous observation of different objects during the digestion. A transition from vesicles to micelles during digestion was evidenced.

More experiments are currently performed to understand this transition, and also the effects of the formulation, as only the type of triglyceride had a clear influence on the digestion in this study.

Acknowledgments

We thank Steven Le Feunteun, Olivier Vitrac of INRA Île-de-France for fruitful discussions, and Jérôme Crassous, Arnaud Saint-Jalmes of IPR Rennes for their help with DWS. The Carnot Institute Qualiment is acknowledged for financial support.

References

1 S. S. Gropper, J. L. Smith and J. L. Groff, *Advanced Nutrition and Human Metabolism*, Wadsworth, Belmont, CA, 5th edn., 2009.

2 S. Marze, accepted in *Crit. Rev. Food Sci. Nutr.*, DOI:10.1080/10408398.2010.525331.

3 D. C. Dawson, Principles of Membrane Transport, *Comprehensive Physiology*, 2011, 1-44.

4 J. Parada and J. M. Aguilera, *J. Food Sci.*, 2007, **72**, R21-R32.

5 D. J. McClements and Y. Li, *Adv. Colloid Interface Sci.*, 2010, **159**, 213-228.

6 Z. Gaygadzhiev, M. Corredig and M. Alexander, *Langmuir*, 2008, **24**, 3794-3800.

7 S. Marze, R. M. Guillermic and A. Saint-Jalmes, *Soft Matter*, 2009, **5**, 1937-1946.

8 A. Stradner, S. Romer, C. Urban and P. Schurtenberger, *Progr. Colloid Polym. Sci.*, 2001, **118**, 136-140.

9 O. Soderman and P. Stilbs, *Prog. Nucl. Mag. Res. Sp.*, 1994, **26**, 445-482.

10 T. M. Squires and T. G. Mason, *Annu. Rev. Fluid Mech.*, 2010, **42**, 413-438.

11 D. P. Cistola, J. A. Hamilton, D. Jackson and D. M. Small, *Biochemistry*, 1988, **27**, 1881-1888.

12 H. J. Kim, E. A. Decker and D. J. McClements, *Langmuir*, 2004, **20**, 10394-10398.

13 W. Brown, *Dynamic Light Scattering*, Clarendon Press, Oxford, 1993.

14 B. J. Frisken, *Appl. Optics*, 2001, **40**, 4087-4091.

15 D. J. Pine, D. A. Weitz, J. X. Zhu and E. Herbolzheimer, *J. Phys. France*, 1990, **51**, 2101-2127.

16 D. A. Weitz and D. J. Pine, in *Dynamic Light Scattering*, ed. W. Brown, Clarendon Press, Oxford, 1993, ch. 16, 652-720.

17 G. K. Batchelor, *J. Fluid Mech.*, 1976, **74**, 1-29.

18 V. Gopal , H. Ramachandran and A. K. Sood, 1999, arXiv:cond-mat/9906227v1.

19 S. Sanyal and A. K. Sood, *Pramana J. Phys.*, 1995, **45**, 1-17.

20 N. A. Mazer, M. C. Carey, R. F. Kwasnick and G. B. Benedek, *Biochemistry*, 1979, **18**, 3064-3075.

21 M. Svard, P. Schurtenberger, K. Fontell, B. Jonsson and B. Lindman, *J. Phys. Chem.*, 1988, **92**, 2261-2270.

22 H. Fukuda, A. Goto, H. Yoshioka, R. Goto, K. Morigaki and P. Walde, *Langmuir*, 2001, **17**, 4223-4231.

23 S. W. Provencher, *Comp. Phys. Commun.*, 1982, **27**, 213-227, 229-242.

24 A. F. Kostko and V. A. Pavlov, *Appl. Optics*, 1997, **36**, 7577-7582.

25 M. J. Saxton, *Biophys. J.*, 1994, 66, 394-401.

26 R. Mezzenga, P. Schurtenberger, A. Burbidge and M. Michel, *Nat. Mater.*, 2005, **4**, 729-740.

27 M. J. Hey and F. Al-Sagheer, *Langmuir*, 1994, **10**, 1370-1376.

28 H. Egger and K. M. McGrath, *J. Colloid Interface Sci.*, 2006, **299**, 890-899.

29 F. Caboi, J. Borne, T. Nylander, A. Khan, A. Svendsen and S. Patkar, *Colloid Surface B*, 2002, **26**, 159-171.

30 M. I. Burgar, P. Hoobin, R. Weerakkody, L. Sanguansri and M. A. Augustin, *Food Biophys.*, 2009, **4**, 32-41.

31 J. W. Goodrum and M. A. Eiteman, *Bioresource Technol.*, 1996, **56**, 55-60.

32 N. C. Exarchos, M. Tasioula-Margari and I. N. Demetropoulos, *J. Chem. Eng. Data*, 1995, **40**, 567-571.

33 Y. Marcus, *J. Phys. Org. Chem.*, 2003, **16**, 398-408.

34 A. F. Hofmann and B. Borgström, *J. Clin. Invest.*, 1964, **43**, 247-257.

35 K. Y. Liew, C. E. Seng and E. K. Lau, *J. Am. Oil Chem. Soc.*, 1991, **68**, 488-492.

36 H. Noureddini, B. C. Teoh and L. Davis Clements, *J. Am. Oil Chem. Soc.*, 1992, **69**, 1184-1188, 1189-1191.

37 P. Stilbs, H. Walderhaug and B. Lindman, *J. Phys. Chem.*, 1983, **87**, 4762-4769.

38 J. Singh, Z. Unlu, R. Ranganathan and P. Griffiths, *J. Phys. Chem. B*, 2008, **112**, 3997-4008.

39 P. Schurtenberger, N. Mazer and W. Kanzig, *J. Phys. Chem.*, 1985, **89**, 1042-1049.

40 A. Walter, P. K. Vinson, A. Kaplun and Y. Talmon, *Biophys. J.*, 1991, **60**, 1315-1325.

41 W. R. Hargreaves and D. W. Deamer, *Biochemistry*, 1978, **17**, 3759-3768.

42 S. Marze and M. Choimet, submitted to *Soft Matter*.

43 Y. Li and D. J. McClements, *J. Agric. Food Chem.*, 2010, **58**, 8085-8092.

44 M. Golding, T. J. Wooster, L. Day, M. Xu, L. Lundin, J. Keogh and P. Clifton, *Soft Matter*, 2011, **7**, 3513-3523.

45 S. Mun, E. A. Decker and D. J. McClements, *Food Res. Int.*, 2007, **40**, 770-781.

46 P. M. Reis, T. W. Raab, J. Y. Chuat, M. E. Leser, R. Miller, H. J. Watzke and K. Holmberg, *Food Biophys.*, 2008, **3**, 370-381.

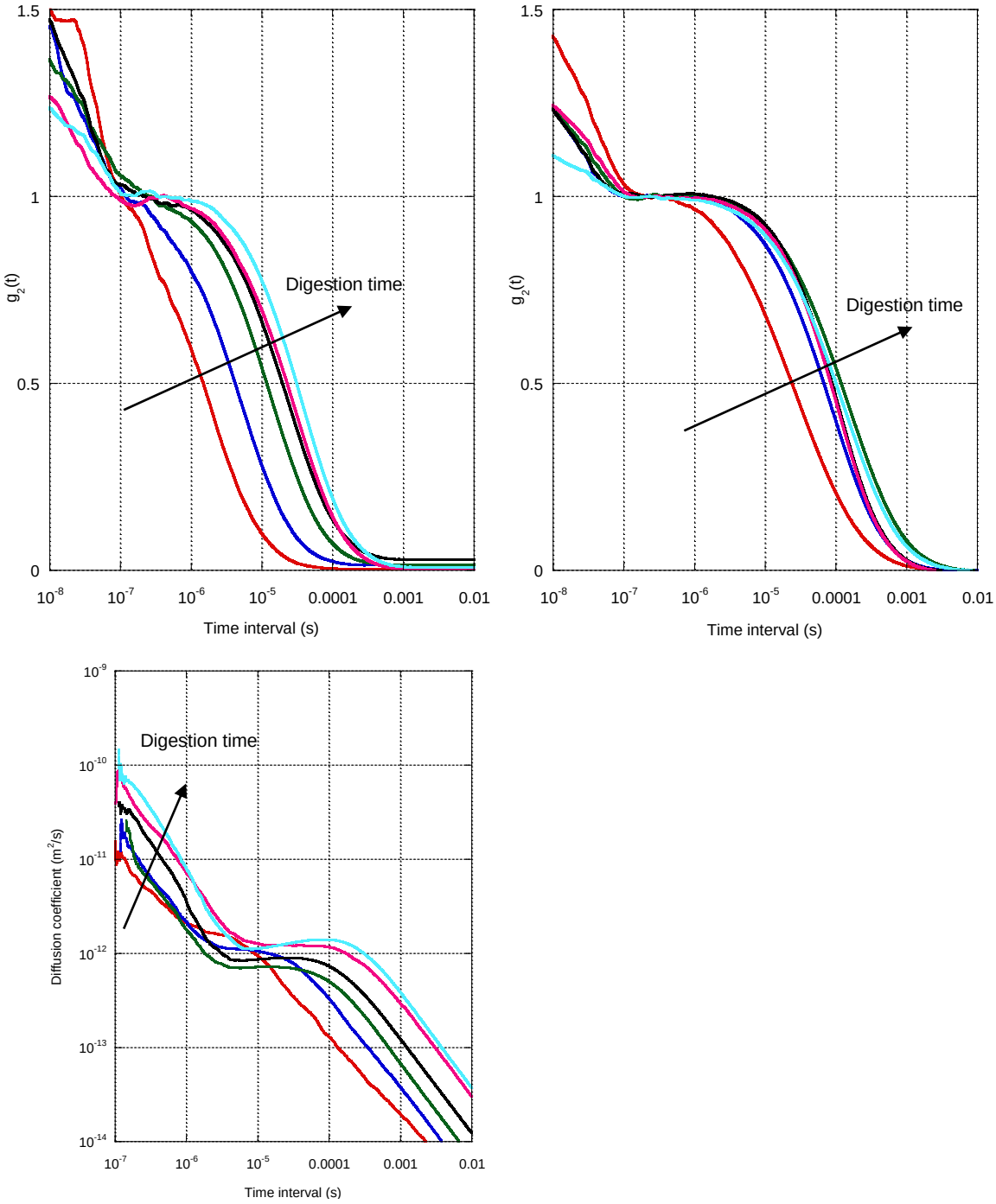

Figure 1: Forward-scattering (left) and back-scattering (right) IACF measured by DWS for a TO-βLG+ emulsion undergoing in vitro digestion. The bottom graph shows the time-resolved diffusion coefficient calculated from the forward-scattering IACF.

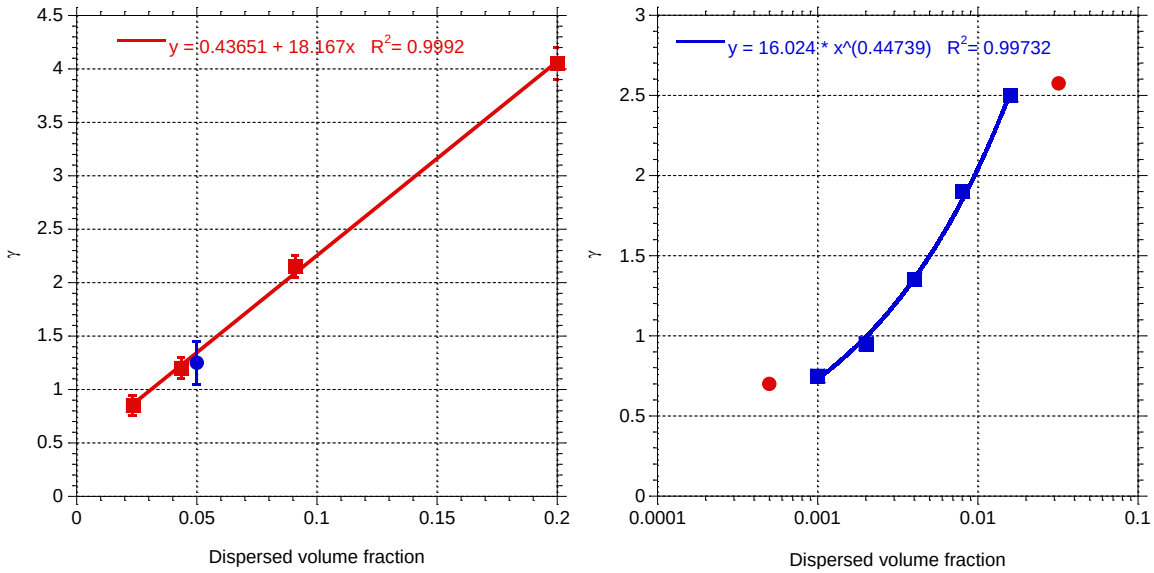

Figure 2: The back-scattering DWS coefficient γ as a function of the dispersed volume fraction for: a TO-βLG emulsion diluted in 100 *mM* NaH_2PO_4 buffer alone at 37 °C (left, square), all reference emulsions in digestion conditions (left, circle), a 200 nm monodisperse polystyrene particles dispersion diluted in water (right, the deviations are within the symbols). Only the squares were used for the fittings.

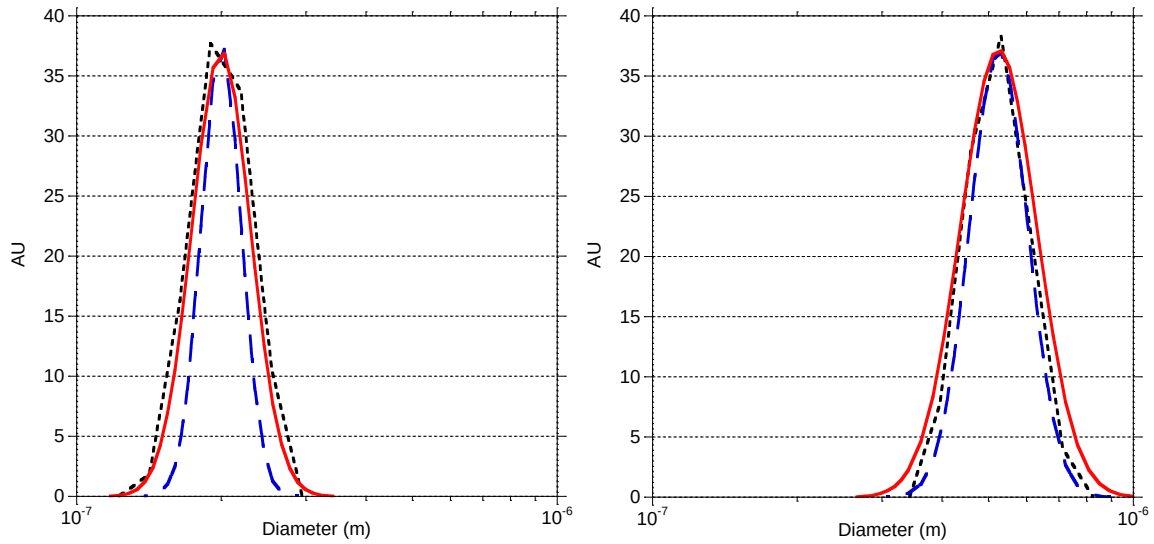

Figure 3: PSD for 200 nm (left, ϕ=0.016) and 500 nm (right, ϕ=0.018) monodisperse polystyrene particles dispersions obtained by DLS (black dotted line, volume-based PSD), back-scattering DWS (blue dashed line) and forward-scattering DWS (red line).

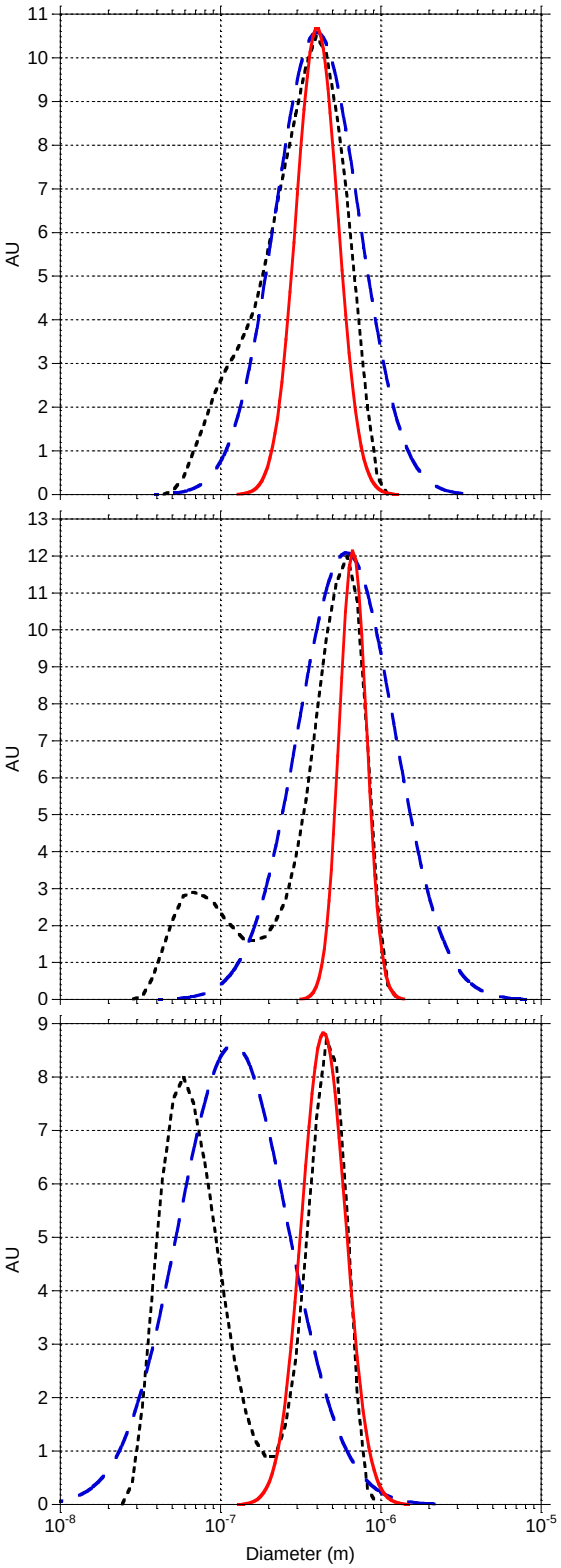

Figure 4: PSD for a TO-βLG+ emulsion during digestion (from top to bottom at 10, 130 and 310 min). Same legend as figure 3.

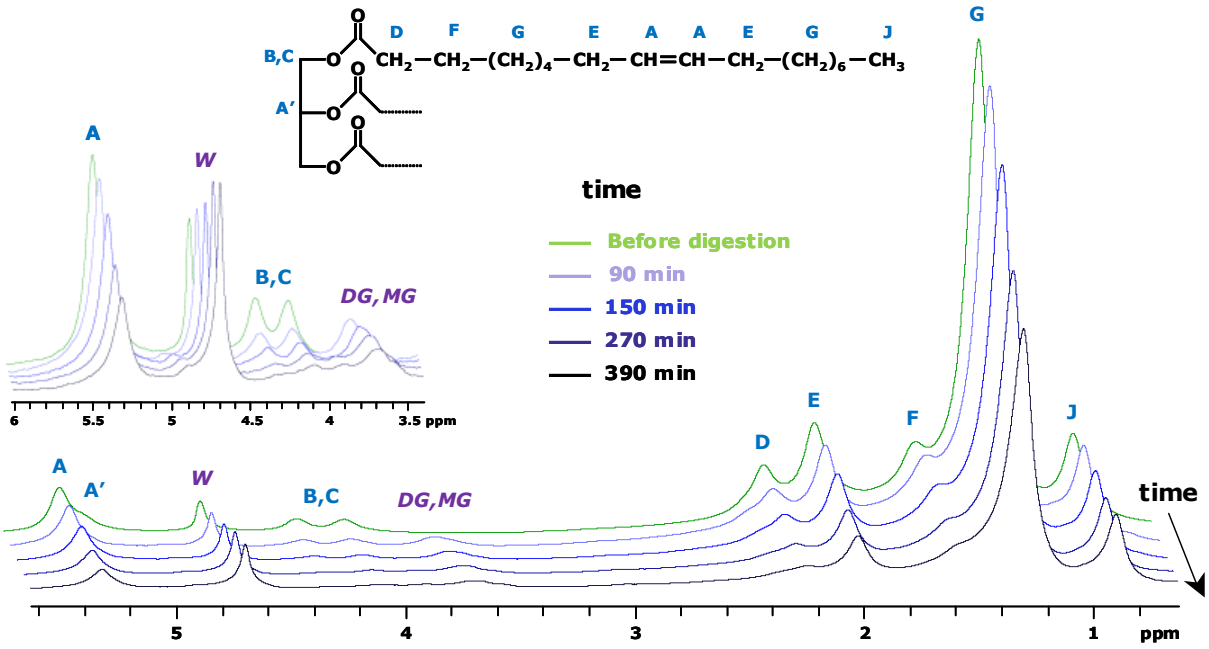

Figure 5: Stacked plot of the evolution of the ^{1}H NMR spectrum for a TO-βLG+ emulsion as a function of digestion time at a gradient strength of 148 $G.cm^{-1}$. The insets show a magnification of the peaks around the water peak (W) and the assignment of the protons on the TO.

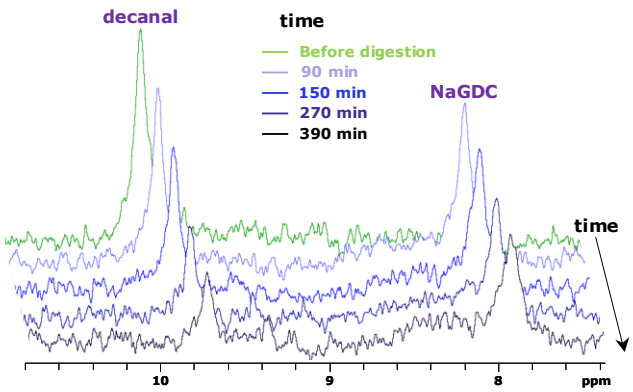

Figure 6: Same as figure 5 in the high chemical shifts region.

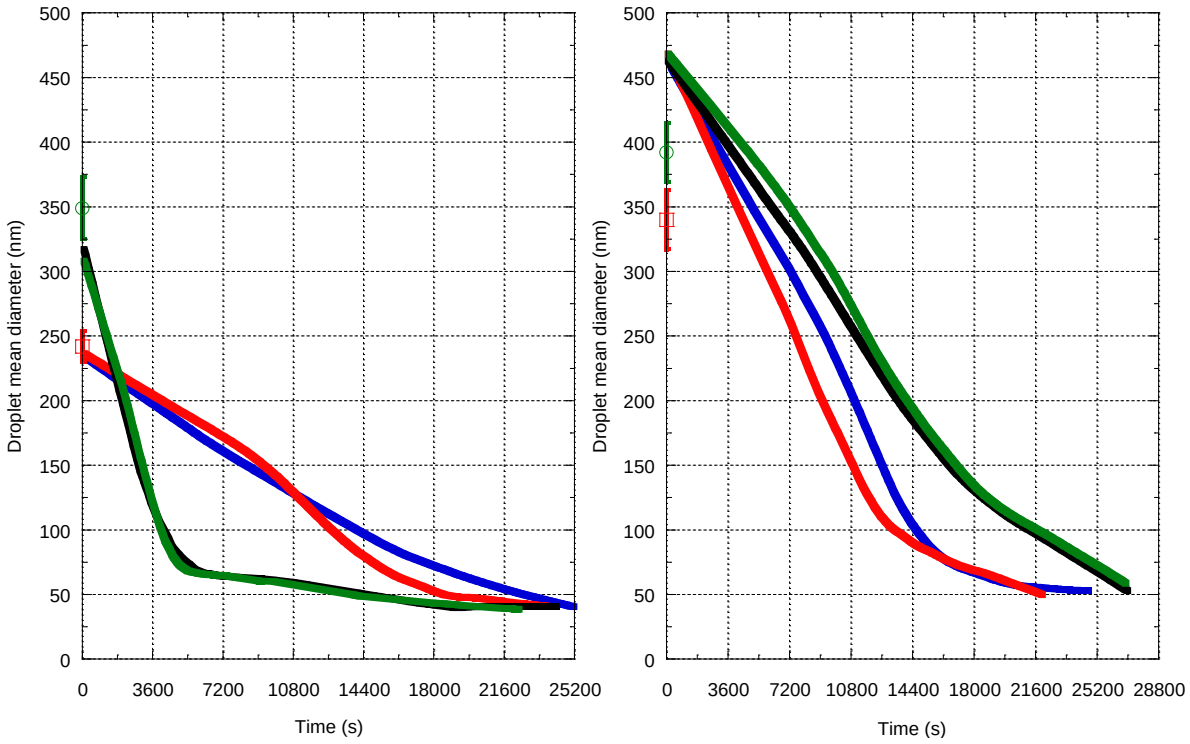

Figure 9: DLS volume-based mean droplet diameter variation during digestion, obtained by averaging the data of two digestions for each emulsion. TC emulsions (left) are NaO, NaO+, βLG+ and βLG, from top to bottom at 7200 s. TO emulsions (right) are βLG, βLG+, NaO+ and NaO, from top to bottom at 7200 s. For clarity, the deviation is not represented. During the first hour, it is about ± 50 nm for TC and ± 100 nm for TO. Then, it is about the line thickness. The symbols represent the LD average surface-based mean droplet diameter for the initial emulsions pre-diluted 4-fold in 130 *mM* NaH_2PO_4 buffer (circle: βLG, square: NaO).

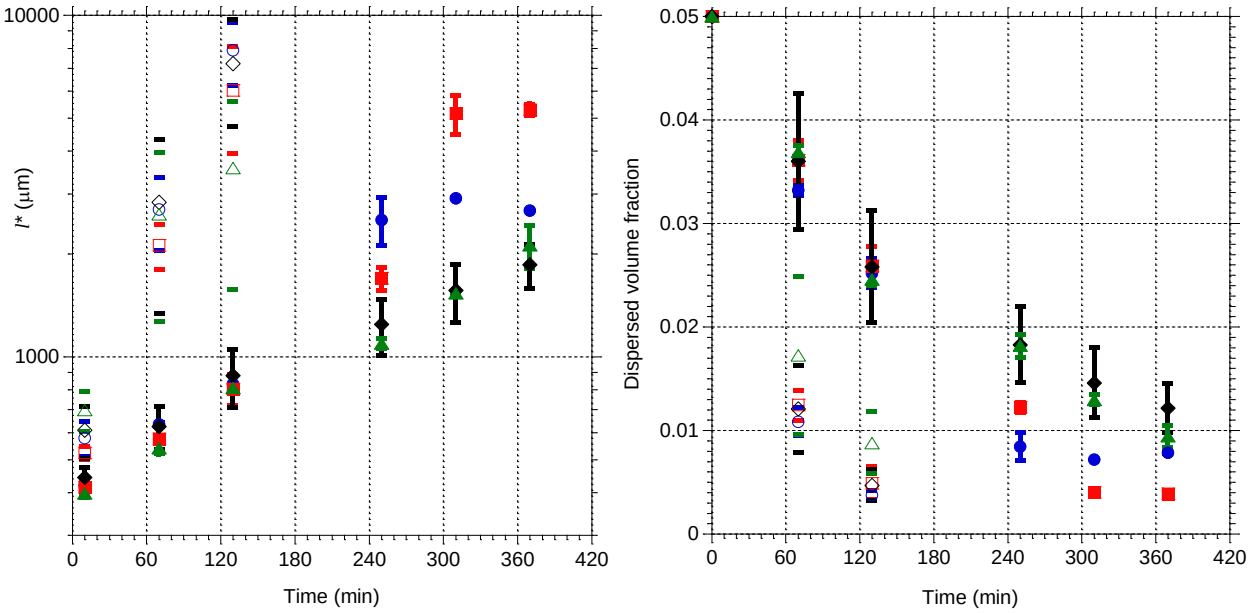

Figure 10: *l** from the forward-scattering DWS measurements, and the deduced dispersed volume fraction as a function of digestion time for TC (open symbols) and TO (filled symbols) emulsions with emulsifier NaO (square), NaO+ (circle), βLG (triangle) and βLG+ (diamond). For clarity, the TC deviations are shown as caps only, visible in the color version of the article.

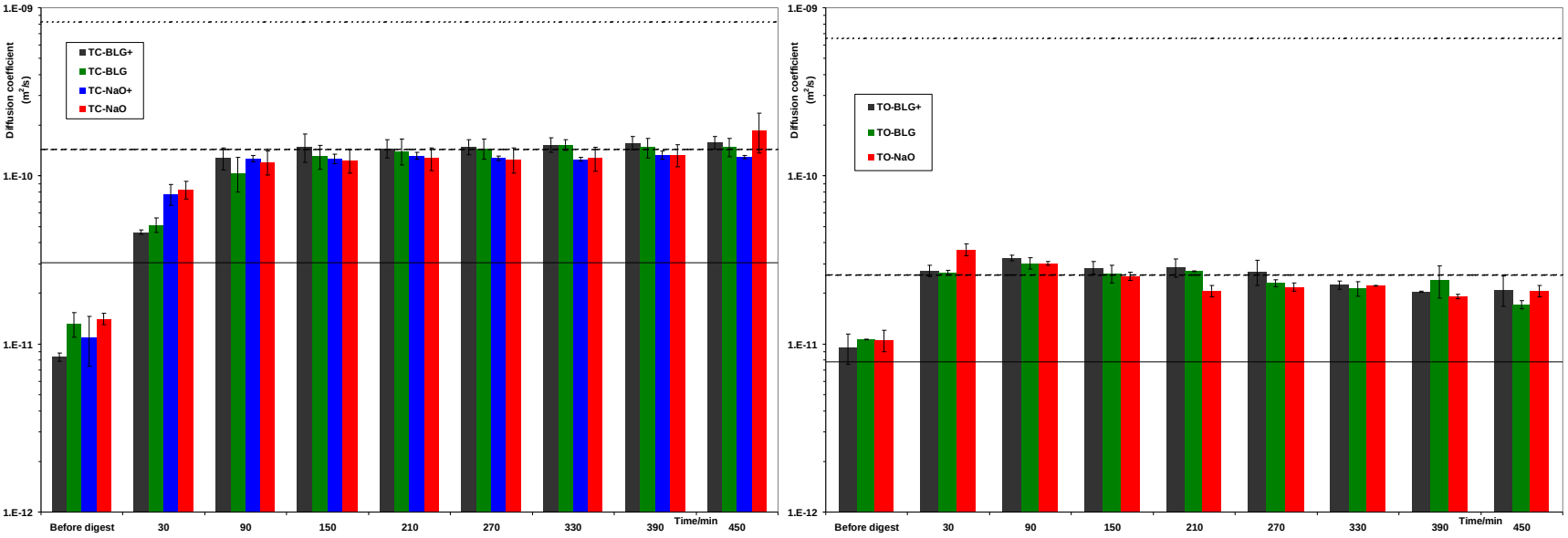

Figure 7: Lipid molecular diffusion coefficient measured by NMR as a function of digestion time for TC (left) and TO (right) emulsions. Lines represent the theoretical diffusion coefficient for TG/TG (thick), FA/FA (dashed) and FA/W (dotted). Emulsifiers are, from left to right: βLG+, βLG, (NaO+), NaO.

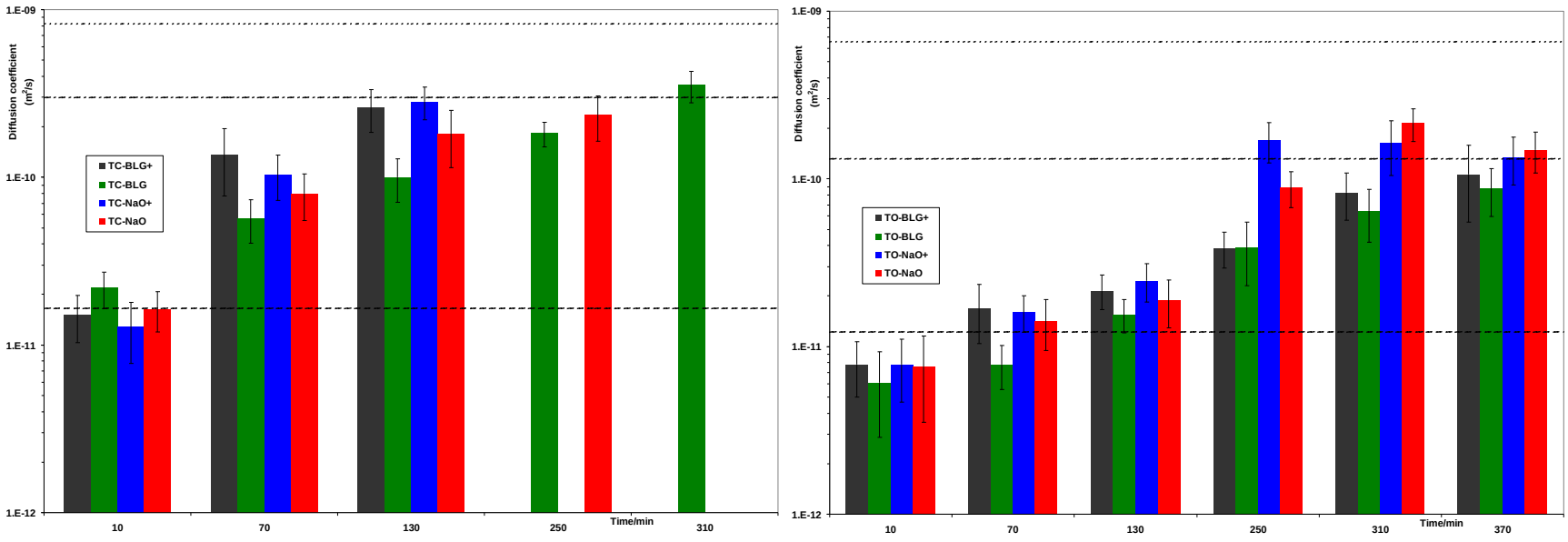

Figure 8: Supramolecular diffusion coefficient measured by DWS as a function of digestion time for TC (left) and TO (right) emulsions. Lines represent the theoretical diffusion coefficient for V/M (dashed), M/W (mixed) and FA/W (dotted). Emulsifiers are, from left to right: βLG+, βLG, NaO+, NaO.